
Microautoradiographic Study for the Differentiation of Intratumoral Macrophages, Granulation Tissues and Cancer Cells by the Dynamics of Fluorine-18-Fluorodeoxyglucose Uptake

Roko Kubota, Kazuo Kubota, Susumu Yamada, Masao Tada, Tatsuo Ido and Nobuaki Tamahashi

Department of Nuclear Medicine and Radiology, and Pharmacology, Institute of Development, Aging and Cancer, Cyclotron and Radioisotope Center, Tohoku University; and Clusterecore Institute of Biology, Sendai, Japan

A substantial amount of macrophage infiltration occurs in both human and animal tumors. We previously showed that 2-deoxy-2-[¹⁸F]fluoro-D-glucose ([¹⁸F]FDG) uptake was higher in tumor-associated macrophages and young granulation tissues than in tumor cells. Differentiation of intratumoral non-neoplastic cells from neoplastic cells is important not only for the reduction of false-positives in FDG-PET tumor studies but also for patient management. **Methods:** A time-course study was performed using micro- and macro-autoradiography and tissue distribution in C3H/He mice bearing transplanted syngeneic FM3A mammary carcinoma and MH134 hepatoma was evaluated to analyze the intratumoral cellular dynamics of [¹⁸F]FDG and 2-deoxy-D-[³H]glucose *in vivo*. **Results:** The volume-doubling time *in vivo* was 1.3 days for MH134 and 4.9 days for FM3A, and the survival time of the host was 32.1 and 40.3 days, respectively. The peak uptake of both tracers in the tumor was 60 min after intravenous injection. The uptake by MH134 was 1.7–2.1 times higher than that by FM3A. The intracellular concentration as determined by counting the silver grains on micro-autoradiographic sections showed that the uptake by macrophages and focal small necrotic areas in both tumors was faster than the blood clearance until 15 min after tracer injection. **Conclusion:** Thus, non-neoplastic cellular elements can be differentiated from viable neoplastic cells by means of the dynamic analysis of [¹⁸F]FDG uptake.

Key Words: fluorine-18-fluorodeoxyglucose; intratumoral macrophages; granulation tissue; cancer cells; microautoradiography

J Nucl Med 1994; 35:104–112

Fluorine-18-2-deoxy-2-fluoro-D-glucose ([¹⁸F]FDG) is a useful tumor-detecting agent (1–4). The mechanism of accumulation of this tracer into malignant tissue is due to the enhanced rate of glucose utilization by neoplastic cells (5–7). Clinical studies using positron emission tomography (PET) have demonstrated that [¹⁸F]FDG can be used to differentiate malignant from benign tumors (8), grade malignancy (9) and to evaluate the proliferative activity of the tumor tissue (10). The high accumulation of [¹⁸F]FDG in the tumor is believed to represent the high metabolic activity of the neoplastic cells (11). However, our recent *in vivo* autoradiographic study (12) also revealed high accumulation of [¹⁸F]FDG in tumor-associated macrophages and in young granulation tissues. We showed that about 24% of the [¹⁸F]FDG utilization in a tumor was due to non-neoplastic cellular elements.

Immunologic effector cells within the tumor, such as T-lymphocytes and macrophages, were found to be of a lower percentage of the human tumor component as determined by histology of conventionally stained tumor sections (13,14). However, recent investigations using cell-surface markers have revealed a substantial amount of macrophage infiltration in many human tumors such as breast cancer (14,15), primary and metastatic melanomas (16), malignant glial tumors (17,18), bone tumors (19), renal cell carcinoma (20), laryngeal carcinomas (21), non-Hodgkin's lymphomas (22) and childhood tumors (23).

Human and animal tumors are characterized by infiltration of macrophages, which frequently constitutes 20%–30% of the cellular tumor mass (14,24). The percentage of macrophages may increase after anti-neoplastic treatment (25–27) because the destruction of tumor cells evokes an enhanced respiratory burst of macrophages (28). This immune reaction of the tumor-bearing host seemed to be the cause of the false-positive tumor cell uptake of [¹⁸F]FDG in post-treatment PET studies performed to assess therapeutic efficacy (27,29). The presence of large numbers of tu-

Received Apr. 8, 1993; revision accepted Sept. 15, 1993.

For correspondence and reprints contact: Roko Kubota, Dept. of Nuclear Medicine and Radiology, Institute of Development, Aging and Cancer, Tohoku University, 4-1 Seiryō-cho, Aoba-ku, Sendai 980, Japan.

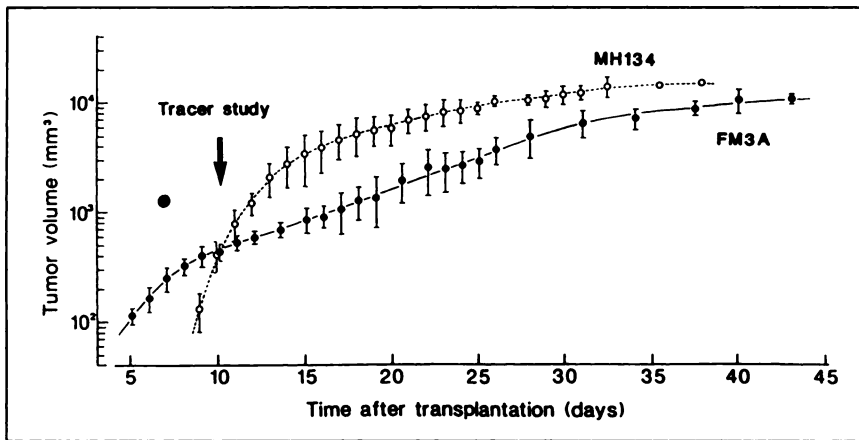


FIGURE 1. Tumor growth curves represented by daily averages of all tumor measurements during the survival time of eight mice each. The day when the tumor cells were transplanted was designated as Day 0.

mor-associated macrophages and their high levels of [^{18}F]FDG accumulation are believed to contribute to the high tumor uptake of [^{18}F]FDG in PET images. Therefore, determining the differential uptake of intratumoral non-neoplastic cells from neoplastic cells by [^{18}F]FDG uptake is important and valuable not only for the reduction of false-positives in FDG tumor studies, but also to improve the accuracy of FDG-PET.

Here, we report the dynamics of [^{18}F]FDG and/or 2-deoxy-D- [^3H]glucose ([^3H]DG) uptake by various cellular elements in two malignant tumor models transplanted into the same syngeneic host mice. Neoplastic and non-neoplastic cellular elements were differentiated.

MATERIALS AND METHODS

The animals were maintained in the animal care facility of our institution and the study protocol was approved by the Laboratory Animal Care and Use Committee of Tohoku University.

Animal Models

Ten-week-old C3H/He female mice were subcutaneously injected with a 0.1-ml suspension of 10^7 syngeneic FM3A mammary carcinoma cells and 10^6 syngeneic MH134 hepatoma cells, respectively, into the left and right thighs. Solid tumors produced on one side of the thighs of eight mice were measured with vernier calipers and the growth curves were drawn as described previously (12,30). Tracer experiments were performed 10 days after tumor transplantation.

Double-Tracer Tissue Distribution Study

Thirty-five mice bearing both FM3A and MH134 tumors were injected intravenously into the lateral tail vein with a mixture of 20 μCi (740 kBq) of [^{18}F]FDG and 1 μCi (37 kBq) of [^3H]DG (Amersham International plc, Buckinghamshire, UK) in 0.2 ml of saline and killed 1, 5, 15, 30, 45, 60 and 120 min later. Tissue samples were excised and weighed, and the ^{18}F radioactivity was measured using an automated gamma-scintillation counter. Three days later (approximately 39 half-lives of ^{18}F), when the ^{18}F radioactivity had decayed, the tissue samples were digested and bleached with perchloric acid and hydrogen peroxide (1:3) in a heater at 80°C . After cooling, the samples were mixed with a scintillation cocktail and left at room temperature overnight, after which ^3H was measured using a liquid scintillation counter (LSC)

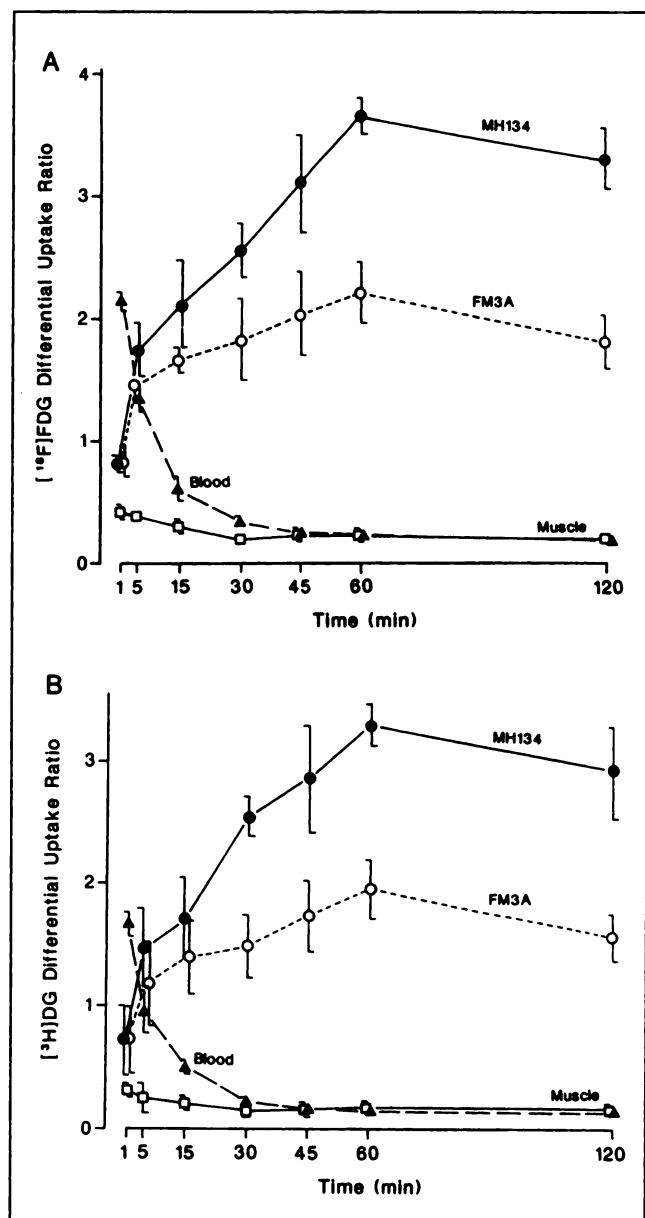


FIGURE 2. Time-course curves for the uptake by MH134 and FM3A tumors, muscles and for the blood levels. Fluorine-18-FDG (A) and [^3H]DG (B) were simultaneously injected into the mice bearing both tumors ($n = 5$ each time after injection).

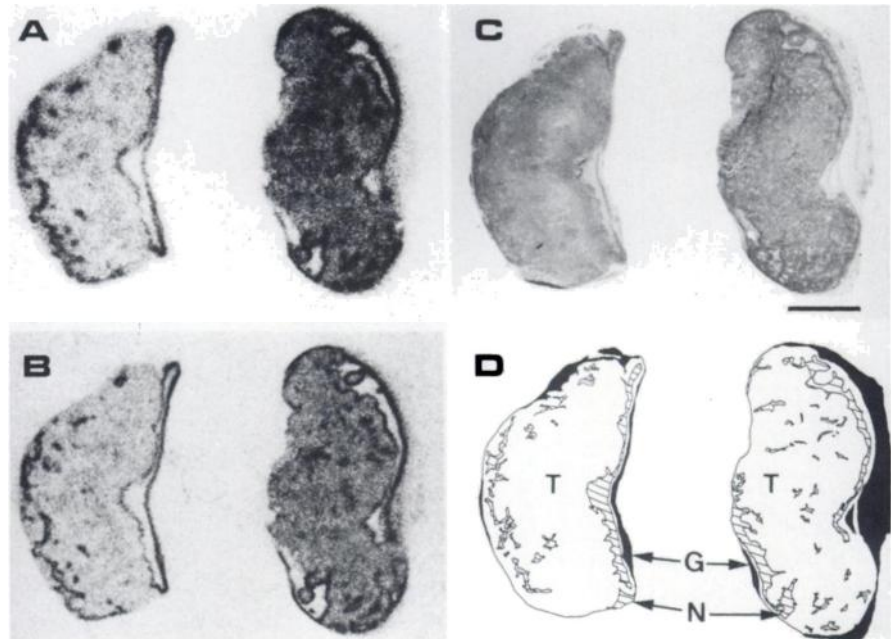


FIGURE 3. A combination of double-tracer macro-autoradiograms and microscopy. Images of [^{18}F]FDG distribution (A) and [^3H]DG (B), a photomicrograph of specimen (C) which produced the autoradiograms, and an illustration of microscopic image (D). Left, FM3A tumor; Right, MH134 tumor; T, tumor cells; G, granulation tissue; N, necrosis. Scale bar: 2 mm.

(31). Tissue radioactivity was expressed as the differential uptake ratio (DUR) (32):

$$\text{DUR} = \frac{\text{tissue counts/tissue weight}}{\text{injected dose counts/body weight}}$$

Double-Tracer Macro-Autoradiography with [^{18}F]FDG and [^3H]DG

Five C3H mice bearing both FM3A and MH134 tumors were injected with a mixture of 200 μCi (7.40 MBq) of [^{18}F]FDG and 20 μCi (740 kBq) of [^3H]DG in 0.2 ml and killed 1 hr later. The tumors were dissected and frozen as reported previously (12). Several 3.5- μm thick sections were mounted on clean glass slides, air-dried and directly placed in contact with ARG film (MARG ^3H -type, Konica, Tokyo, Japan) for 2 hr to produce [^{18}F]FDG images. Three days later, the same sections were placed in contact with separate films for 8 wk to produce [^3H]DG images.

Time-Course Macro- and Micro-Autoradiography with [^3H]DG

Twenty-six mice bearing both FM3A and MH134 tumors were injected intravenously with 20 μCi (740 kBq) of [^3H]DG in 0.2 ml saline and killed 1, 5, 15, 30, 45 and 60 min later. The tumors were quickly removed, cut into frozen sections, then 3.5- μm thick sections were processed for micro-autoradiography (12). After exposure for 2 wk, the sections were developed, fixed and stained with hematoxylin and eosin. Nonradioactive tumor sections were processed in the same manner as chemographic controls. The silver grains were counted in various tumor regions under a transmitted light brightfield microscope using a micrometer. The analyses were performed blindly. The grain distribution of [^3H]DG in the tumor tissue was similar to that of [^{18}F]FDG in our previous study (12).

The contiguous 3.5- μm thick sections from the same frozen blocks used in the micro-autoradiographic study were mounted on clean glass slides and air-dried. All 26 samples were simultaneously arranged in a film cassette and exposed to ARG film for 8 wk to visualize the [^3H]DG distribution under the same condi-

tions. After the exposure, the sections were stained with hematoxylin and eosin.

Quantitative Analysis

To determine the film response to ^{18}F and ^3H radioactivity, and the relationship between micro-autoradiographic grain numbers and ^3H radioactivity, normal female C3H/He mice were injected intravenously with [^{18}F]FDG in various doses from 0.1 to 8 mCi, or [^3H]DG in doses of 10 to 50 μCi , then killed 1 min later. The 3.5- μm thick liver sections were then processed for ARG as uniform step-wedge standards of radioactive samples. The film response was determined after various exposure periods and the optical grain density was measured with a densitometer. The micro-autoradiograms were developed after a 2-wk exposure, counterstained with eosin and the grain numbers per unit area were counted as described above. The radioactivities per unit area of the sections were measured with a gamma-counter and corrected for decay for ^{18}F (12) and with a LSC for ^3H (31).

RESULTS

Tumor Growth Curves

The growth curves of subcutaneously transplanted FM3A and MH134 tumors are shown in Figure 1. The growth rate of the MH134 tumor was faster than that of FM3A tumor. The volume doubling time of the tumor in vivo was about 1.3 and 4.9 days for MH134 and FM3A respectively, when the tracer experiment was performed 10 days after transplantation. The mean survival time after transplantation was 32.1 ± 6.7 and 40.3 ± 5.0 days for MH134 and FM3A, respectively.

Time Course and Tissue Distribution

The uptake by MH134 and FM3A tumors, muscle and blood were studied from 1 to 120 min after a simultaneous injection of [^{18}F]FDG and [^3H]DG (Fig. 2). Both tracers had the same uptake profile in the tissues. Tumor uptake increased rapidly for the first 5 min after injection, then

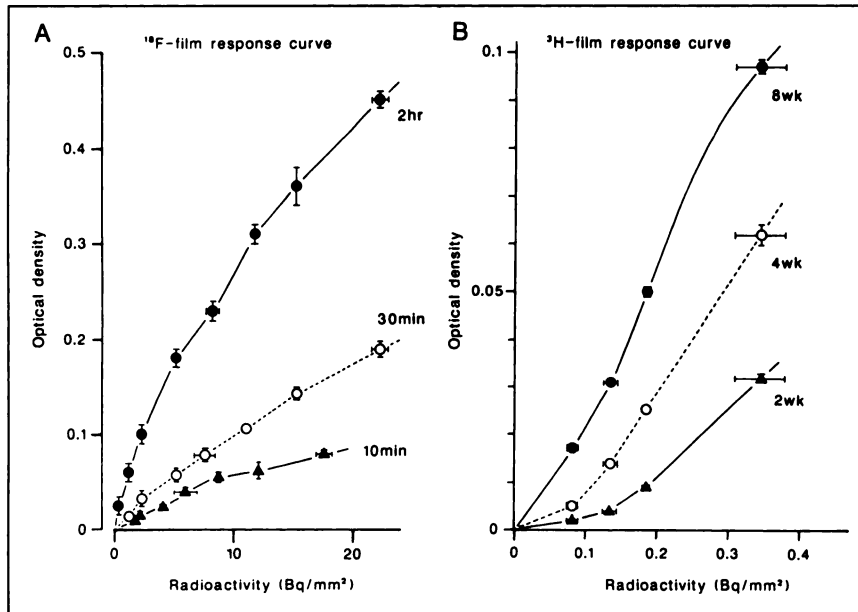


FIGURE 4. Response curves of macroautoradiographic film (MARG ^3H -type, Konica, Japan) to ^{18}F (A) and ^3H (B). The responses were examined after 10 min, 30 min and 2 hr for ^{18}F , and 2, 4 and 8 wk for ^3H . The radioactivity plotted was the value when the exposure was started. The difference in the density scales was caused by the different track lengths of each particle.

gradually reached a peak after 1 hr. The uptake by MH134 was 1.7–2.1-fold higher than that by FM3A. Muscle had the lowest uptake which remained constant up to 2 hr. The radioactivity levels in the blood were the highest 1 min postinjection, then decreased rapidly to those seen in muscle. The DUR of [^3H]DG was $18.6\% \pm 7.4\%$ lower than that of [^{18}F]FDG.

Double-Tracer Autoradiograms with [^{18}F]FDG and [^3H]DG

Figure 3 shows typical autoradiograms of a section of both MH134 and FM3A tumors 1 hr after the injection of a mixture of [^{18}F]FDG and [^3H]DG. The autoradiograms of both tracers in both tumors revealed a heterogeneous grain

distribution. The grain density was higher in MH134 than in FM3A. Markedly dense areas were seen at the periphery of the tumors. Translucent areas of no or few grains were seen beneath the markedly dense areas. The other dense spots were distributed throughout the tumors in areas of relatively lower homogeneous density.

The markedly dense areas were macrophage layers and the dense spots were multifocal small necrotic areas. Young granulation tissues were included in the marginal dense area but they were not readily distinguishable in MH134. The relatively lower homogeneous dense areas were tumor cell regions and the grain-free areas were extensive necrotic tissues. A combination of autoradiography of [^{18}F]FDG and [^3H]DG and light microscopy revealed that both tumor tissues were composed of the same tissue elements with a similar tracer distribution. The visual difference in the grain density in the two autoradiograms was caused by the film responses to the physical characteristics of ^{18}F and ^3H (Fig. 4). The contrast of optical density with radioactivity became greater with longer exposure for both tracers. However, autoradiographic quantitation can be achieved using these film-response curves.

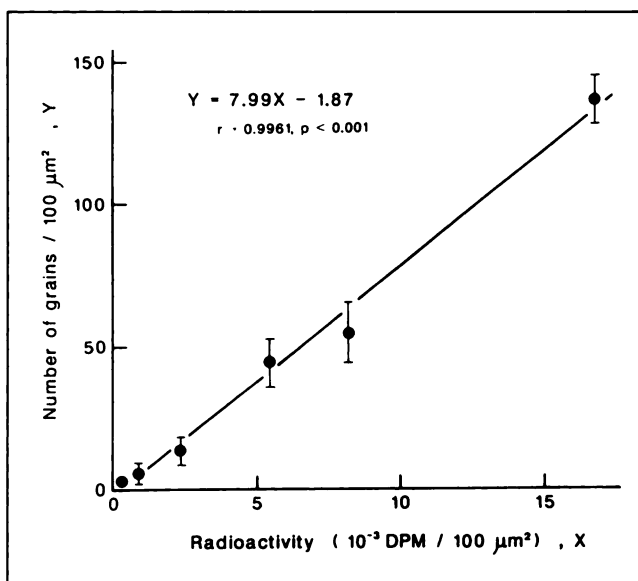


FIGURE 5. A standard curve of the relationship between silver grain numbers and ^3H radioactivity in micro-autoradiography.

Standard Curve for [^3H]DG Microautoradiography

There was a very high correlation between the number of silver grains and the [^3H]DG radioactivity ($y = 7.99x - 1.87$, $r = 0.9961$, $p < 0.001$) (Fig. 5). A microautoradiographic study was performed within the confirmed range of linearity. Silver grains were seen in all tumor sections, and there were no grains in the control sections, thus ruling out the possibility of a positive chemogram.

Time Course of the Uptake of [^3H]DG at the Cellular Level

The silver grain density in various cellular elements of MH134 and FM3A tumor tissues was studied by means of

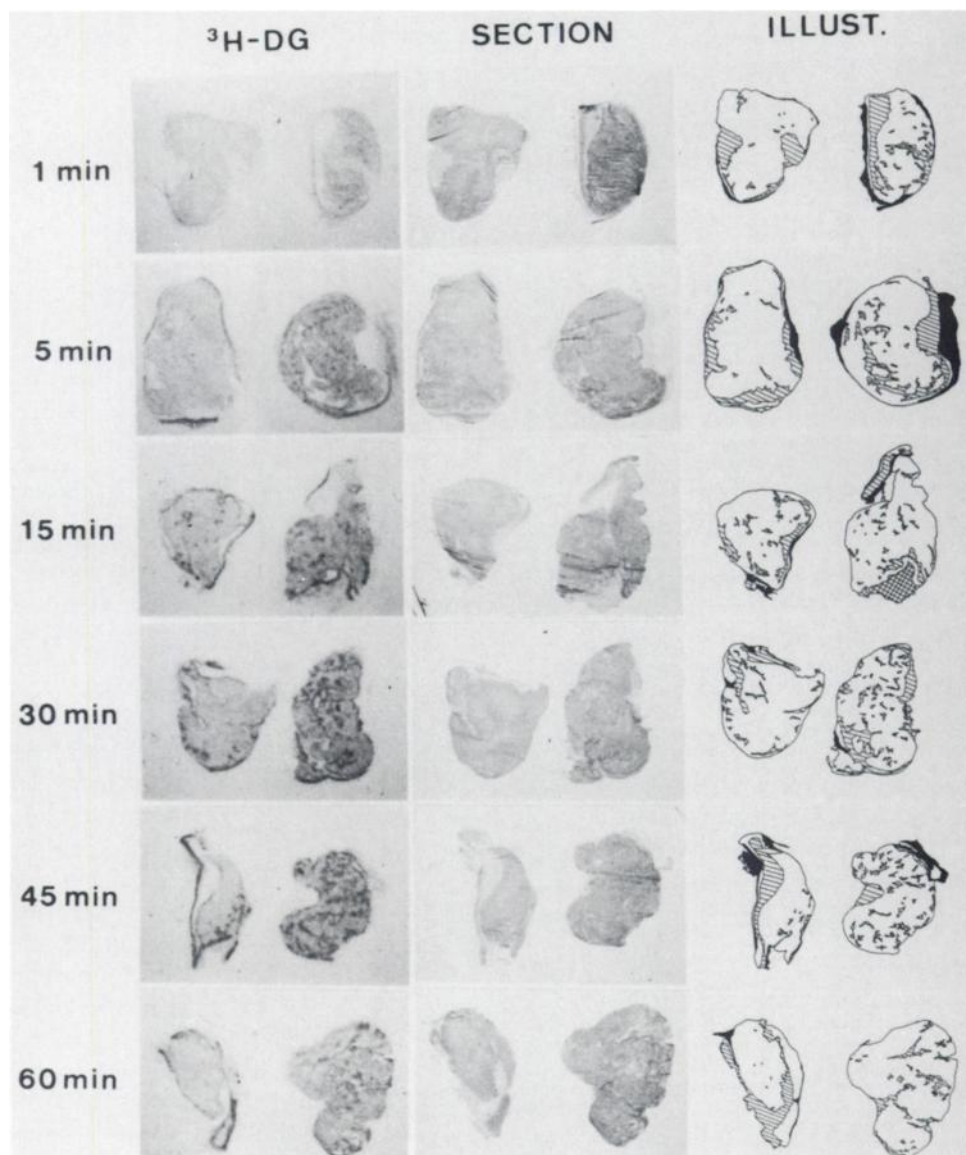


FIGURE 6. The time-course of macro-autoradiographic [^3H]DG distribution in contiguous tumor sections. Shown are micro-autoradiograms and photomicrograms of the section, as well as illustrations. See Figure 3 for other definitions. Left, FM3A tumor; Right, MH134 tumor.

microautoradiography for 1–60 min after injection of [^3H]DG. A typical macro-autoradiogram of contiguous tumor sections by time-course micro-autoradiography is shown in Figure 6. A homogeneous low density area, which corresponded to a viable tissue region and a translucent area of necrosis were seen 1 min after injection. The heterogeneity of grain distribution within the tissue was evident for the next 30 min and remained unchanged for 60 min. MH134 showed higher grain density than FM3A at all time periods.

Figure 7 shows the micro-autoradiographic results of silver grain distribution of [^3H]DG in MH134 and FM3A tissues at the cellular level showing the [^3H]DG uptake in intratumoral cellular elements. Tumor tissue components of interest with various silver grain densities were histologically identified as follows:

1. A layer of macrophages, naturally contaminated with a few microphages, which were massively infiltrating

the marginal areas of extensive tumor necrosis at the periphery of the tumors;

2. A focal necrotic area of less than $30\ \mu\text{m}$ in minimal diameter;
3. Young granulation tissue consisting of capillary vessels, fibroblasts, and phagocytes surrounding tumor mass demarcating the intact host tissue; and
4. A layer of viable tumor cells.

In both MH134 and FM3A, macrophage layers had the highest uptake, which rapidly increased up to 15 min after injection and thereafter became slower. The focal small necrotic area showed the second highest uptake which peaked at 30 min. The uptake in the new granulation tissues was slower and reached a plateau at 30 min. MH134 cells showed higher uptake than FM3A cells and a gradual increase until 60 min.

To examine whether non-neoplastic cellular elements and neoplastic cells can be differentiated by the uptake

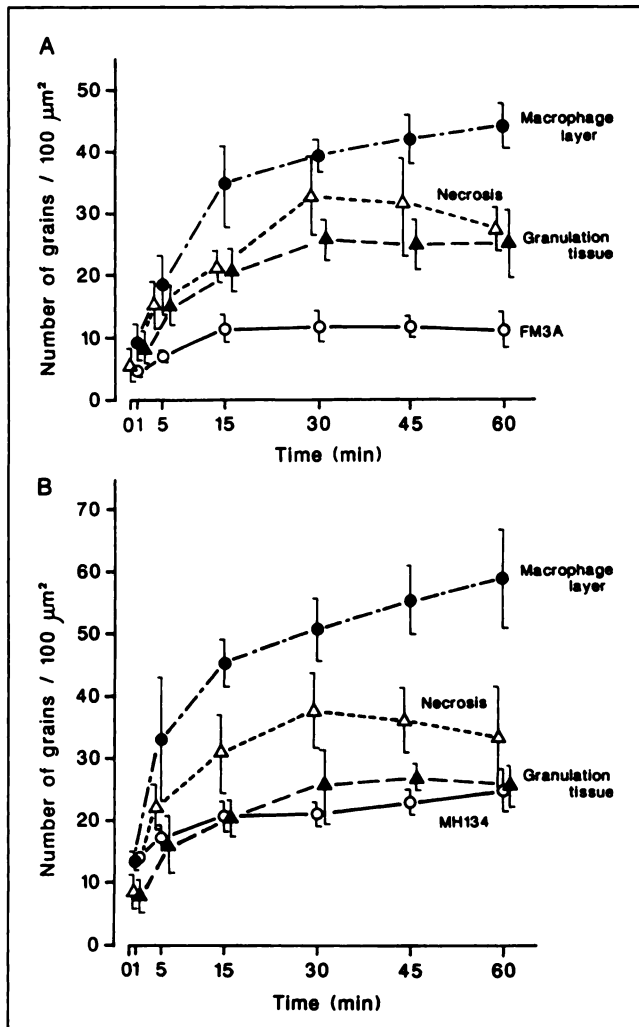


FIGURE 7. The [^3H]DG uptake in intratumoral cellular components of FM3A (A) and MH134 (B) tissues determined by microautoradiographic silver grain counting. Four to five mice with both FM3A and MH134 tumors were studied at each time after injection. The grain numbers in the granulation tissues of both tumors are exactly the same. Necrosis = focal necrotic areas.

dynamics, the grain numbers were compared with the blood clearance (Tables 1–3). The blood level reduced to 1/1.75 at 5 min and 1/3.30 at 15 min compared with the value at 1 min. To compare the rates of blood clearance with the cellular accumulation, we introduced the reciprocal ratio of the blood level to that at 1 min, e.g., 1.75 at 5 min, as the blood clearance ratio, and the ratio of the grain number of each component to that at 1 min as the cellular accumulation ratio. The accumulation ratios of all non-neoplastic cellular elements (macrophage layer, granulation tissue and small necrotic area) were over 1.87 (to 2.70) in both tumors at 5 min. They were higher than the blood clearance ratio (1.75) while the ratios of FM3A (1.54) and MH134 tumor cells (1.26) were lower. The ratios of the macrophage layer (3.79 in FM3A and 3.48 in MH134) and the small necrotic area (3.78 and 3.65) were still higher than the blood clearance ratio (3.30) at 15 min. The ratios of

granulation tissues (2.58 in both tumors) became lower and those of both tumor cells remained lower at 15 min. The ratios of all cellular elements became lower than the blood clearance ratio (>7.53) at 30 min and later.

Additional cellular characteristics of tracer uptake were as follows. The number of grains in MH134 tumor cells were 1.8–3.0 times higher than those in FM3A. The granulation tissues of both MH134 and FM3A tumors showed exactly the same grain numbers in the time course study. The grain numbers in granulation tissues became the same as those of tumor cells in MH134 at 60 min. The increase of grain numbers in the macrophage layer was greater in MH134 than FM3A but was suppressed time-dependently. The accumulation of tracer into the small necrotic area was higher in MH134 but the clearance profile was the same in both tumors.

DISCUSSION

Our data showed that non-neoplastic cellular elements can be differentiated from viable neoplastic cells in the early stage by tracer uptake kinetics in mice bearing two transplanted tumors. The uptake in the macrophage layer and small necrotic regions showed greater changes in the rate of uptake than the blood clearance rate at 5 and 15 min. Granulation tissues showed a greater change at only 5 min. The tumor cells had fewer changes throughout. These differences in early dynamics were observed in both types of tumors, regardless of their different growth rates and glucose utilization levels. The early stage of dynamics may represent the contributions from a combination of factors, such as blood flow, diffusion, and membrane transport of tracers. Each cellular element in the tumors may have a different degree and rate of tracer permeability.

If non-neoplastic and neoplastic cells can be differentiated by early tracer dynamics, false-positives will be reduced. Also, this would enable the metabolic characteristics of macrophages in tumors to be investigated noninvasively. Most malignant tumors contain a variable but substantial number of macrophages (15). High macrophage infiltration may be an indicator of a more aggressive tumor type (16,21). The maturation and activation of tumor-associated macrophages have the potential to affect tumor growth. Their roles are, however, controversial due to the potential of activated macrophages to produce various factors which can either inhibit or enhance tumor growth (24,33). Stimulation of glycolysis is an activation signal of macrophages (34). The glucose utilization by macrophages was 2–4 times higher than that of tumor cells. The contribution of tracer uptake by these macrophages may not be negligible, therefore the investigation of metabolic characteristics of tumor-associated macrophages is important when interpreting FDG-PET results for tumor evaluation and patient management.

Some relationships between tumor, macrophages and the host system were found in this study in the later stage of tracer uptake dynamics. The uptake in macrophages in-

TABLE 1
Silver Grain Distribution of [³H]DG in FM3A Tumor Tissues

FM3A	1 min	5 min	15 min	30 min	45 min	60 min
Number of tumors	4	4	5	4	5	4
Tumor cells (TC)						
Grain numbers/100 μm ²	4.54 ± 0.76*	7.03 ± 1.11 [†]	11.53 ± 2.28	11.76 ± 2.51	11.60 ± 1.80	11.00 ± 3.20
Ratio to TC (1 min)	1.00	1.54	2.53	2.59	2.56	2.42
Macrophage layer (ML)						
Grain numbers/100 μm ²	9.18 ± 2.84 [‡]	18.35 ± 4.80 ^{‡§}	34.81 ± 7.16 [¶]	39.20 ± 2.62 [¶]	41.96 ± 3.94 [¶]	44.09 ± 3.54 [¶]
Ratio to ML (1 min)	1.00	2.00	3.79	4.27	4.57	4.80
Ratio to respective TC	2.02	2.61	3.02	3.33	3.62	4.01
Focal necrosis (N)						
Grain numbers/100 μm ²	5.67 ± 2.63*	15.30 ± 3.94 ^{‡§}	21.42 ± 2.36 [¶]	32.97 ± 6.39 [¶]	31.05 ± 8.02 ^{**}	27.44 ± 3.65 [¶]
Ratio to N (1 min)	1.00	2.70	3.78	5.81	5.48	4.84
Ratio to respective TC	1.23	2.18	1.86	2.80	2.68	2.49
Difference from N (1 min)	0	9.63	15.75	27.30	25.38	23.79
Granulation tissue (G)						
Grain numbers/100 μm ²	8.05 ± 2.70 [‡]	15.02 ± 3.31 ^{‡‡‡}	20.77 ± 3.54 ^{‡‡}	25.73 ± 3.22 [¶]	24.83 ± 4.15 [¶]	25.00 ± 5.94 ^{**}
Ratio to G (1 min)	1.00	1.87	2.58	3.20	3.08	3.11
Ratio to respective TC	1.77	2.14	1.80	2.19	2.14	2.27

Each grain count is the mean ± s.d. in the tumors. Fifteen to 25 microgrid areas in a tumor component were counted and averaged for each point.

*p < 0.01.

[†]p < 0.1.

[‡]p < 0.05, compared to the other study times in each tumor component.

^{‡‡}p < 0.05, ^{‡‡‡}p < 0.001, ^{**}p < 0.01, ^{††}p < 0.005 compared to TC in each time.

creased at a higher rate than in the tumor cells. When both tumors in the same host were compared, the increase of tracer uptake by macrophages was greater in MH134, which also showed a higher tumor growth rate, a higher glucose utilization level and induced a shorter survival of the host than FM3A. The higher metabolic activity of macrophages, as well as their infiltration (16,21) suggests more aggressive

characteristics of tumors. The metabolic activity of macrophages may in some way be regulated by the tumor itself. Fibroblast growth factor is one macrophage-produced growth-inducing factor (33). However, the uptake level and dynamics of granulation tissues were exactly the same in both tumors. This means that the activity of peripheral young granulation tissues of the same aged tumors in the same host

TABLE 2
Silver Grain Distribution of [³H]DG in MH134 Tumor Tissues

MH134	1 min	5 min	15 min	30 min	45 min	60 min
Number of tumors	4	4	5	4	5	4
Tumor cells (TC)						
Grain numbers/100 μm ²	13.70 ± 1.54*	17.21 ± 2.07 [†]	20.57 ± 2.55	21.09 ± 1.91	22.90 ± 1.97	24.96 ± 3.55
Ratio to TC (1 min)	1.00	1.26	1.50	1.54	1.67	1.82
Macrophage layer (ML)						
Grain numbers/100 μm ²	13.03 ± 1.88*	33.03 ± 10.55 [†]	45.37 ± 3.88 [‡]	50.77 ± 5.14 [‡]	55.42 ± 5.70 [‡]	59.20 ± 10.72 [‡]
Ratio to ML (1 min)	1.00	2.53	3.48	3.90	4.25	4.54
Ratio to respective TC	0.95	1.92	2.21	2.41	2.42	2.37
Focal necrosis (N)						
Grain numbers/100 μm ²	8.39 ± 3.61 ^{§¶}	22.15 ± 3.77 [†]	30.67 ± 6.42 [¶]	37.62 ± 6.11 ^{††}	36.15 ± 5.32 ^{**}	33.40 ± 8.21
Ratio to N (1 min)	1.00	2.64	3.65	4.48	4.31	3.98
Ratio to respective TC	0.61	1.29	1.49	1.78	1.58	1.34
Difference from N (1 min)	0	13.76	22.28	29.23	27.76	25.01
Granulation tissue (G)						
Grain numbers/100 μm ²	7.87 ± 2.70 ^{††}	15.67 ± 4.11 [†]	20.33 ± 3.04	25.58 ± 6.36	26.87 ± 2.41 [¶]	25.10 ± 3.41
Ratio to G (1 min)	1.00	1.99	2.58	3.25	3.41	3.19
Ratio to respective TC	0.57	0.91	0.99	1.21	1.17	1.01

Each grain count is the mean ± s.d. in the tumors. Fifteen to 25 microgrid areas in a tumor component were counted and averaged for each point.

*p < 0.05, [†]p < 0.1, [‡]p < 0.005, compared to the other study times in each tumor component.

^{‡‡}p < 0.001, [‡]p < 0.05, ^{††}p < 0.01, ^{**}p < 0.005, compared to TC in each time.

TABLE 3
 $[^3\text{H}]\text{DG}$ Concentration in the Blood of C3H/He Mice Bearing FM3A and MH134 Tumors

Blood level (BL)	1 min	5 min	15 min	30 min	45 min	60 min
DUR*	1.676 ± 0.101 [†]	0.958 ± 0.188 [‡]	0.508 ± 0.055 [§]	0.223 ± 0.026 [¶]	0.174 ± 0.009	0.157 ± 0.028
Ratio to BL (1 min)	1.00	1/1.75	1/3.30	1/7.53	1/9.63	1/10.71
Blood clearance ratio**	1.00	1.75	3.30	7.53	9.63	10.71

*Differential uptake ratio. Mean ± s.d. of five mice.

[†]p < 0.001 compared to 5 min.

[‡]p < 0.005 compared to 15 min.

[§]p < 0.001 compared to 30 min.

[¶]p < 0.05 compared to 45 min.

**The reciprocal value of the ratio to BL (1 min).

were highly regulated by the host immune system, independent of the difference in tumor types.

The tracer distribution in humans may differ slightly from that in mice. However, the difference in $[^{18}\text{F}]\text{FDG}$ uptake dynamics in macrophages and granulation tissues from neoplastic cells is considered to be a common biological phenomenon. These data indicate the possibility of identifying false-positives in FDG-PET oncology studies and we also believe that this methodology will be useful for evaluating local immunological reactions by FDG-PET using pixel-by-pixel-based computation.

ACKNOWLEDGMENTS

The authors thank Dr. Prantika Som, Brookhaven National Laboratory for advice; the staffs of the Cyclotron and Radioisotope Center, Tohoku University, for their cooperation; and Mr. Y. Sugawara for photography. This work was supported by grants-in-aid (03454277 and 04557047) from the Ministry of Education, Science and Culture, Japan.

REFERENCES

- Som P, Atkins HL, Bandyopadhyay D, et al. A fluorinated glucose analog, 2-fluoro-2-deoxy-D-glucose (F-18): nontoxic tracer for rapid tumor detection. *J Nucl Med* 1980;21:670-675.
- Larson SM, Weiden PL, Grunbaum Z, et al. Positron imaging feasibility studies. II. Characteristics of 2-deoxyglucose uptake in rodent and canine neoplasms: concise communication. *J Nucl Med* 1981;22:875-879.
- Di Chiro G, DeLaPaz RL, Brooks RA, et al. Glucose utilization of cerebral gliomas measured by $[^{18}\text{F}]\text{-fluoro-deoxyglucose}$ and positron emission tomography. *Neurology* 1982;32:1323-1329.
- Yonekura Y, Benua RS, Brill AB, et al. Increased accumulation of 2-deoxy-2- $(^{18}\text{F})\text{fluoro-D-glucose}$ in liver metastases from colon carcinoma. *J Nucl Med* 1982;23:1133-1137.
- MacKeehan WL. Glycolysis, glutaminolysis and cell proliferation. *Cell Biol Int Rep* 1982;6:635-650.
- Weber G, Morris HP, Love WC, Ashmore J. Comparative biochemistry of hepatomas. II. Isotope studies of carbohydrate metabolism in Morris hepatoma 5123. *Cancer Res* 1961;21:1406-1411.
- Weber G. Enzymology of cancer cells. *N Engl J Med* 1977;296:541-551.
- Kubota K, Matsuzawa T, Fujiwara T, et al. Differential diagnosis of lung tumor with positron emission tomography: a prospective study. *J Nucl Med* 1990;31:1927-1933.
- Di Chiro G. Positron emission tomography using $[^{18}\text{F}]\text{-fluoro-deoxyglucose}$ in brain tumors, a powerful diagnostic and prognostic tool. *Inves Radiol* 1987;22:360-371.
- Minn H, Joensuu H, Ahonen A, Klemi P. Fluoro-deoxyglucose imaging: a method to assess the proliferative activity of human cancer in vivo. Com-

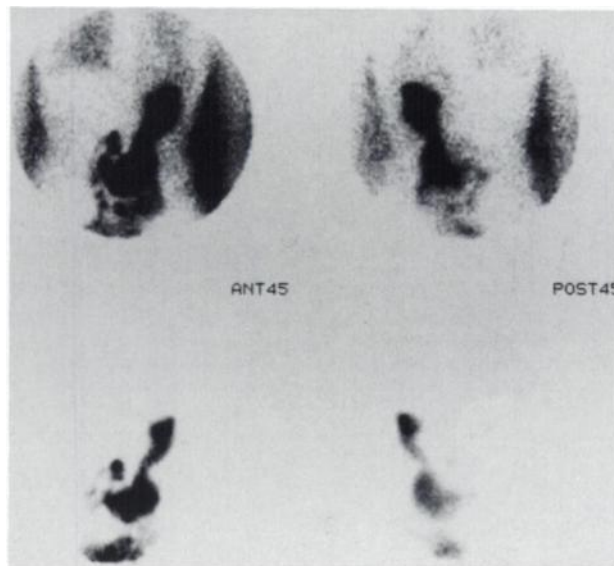
parison with DNA flow cytometry in head and neck tumors. *Cancer* 1988; 61:1776-1781.

- Paul R, Johansson R, Kellokumpu-Lehtinen P-L, Soderstrom K-O, Kangas L. Tumor localization with ^{18}F -2-fluoro-2-deoxy-D-glucose: comparative autoradiography, glucose 6-phosphatase histochemistry, and histology of renally implanted sarcoma of the rat. *Res Exp Med* 1985;185:87-94.
- Kubota K, Yamada S, Kubota K, Ishiwata K, Tamahashi N, Ido T. Intratumoral distribution of fluorine-18-fluoro-deoxyglucose in vivo: high accumulation in macrophages and granulation tissues studied by microautoradiography. *J Nucl Med* 1992;33:1972-1980.
- Underwood JC. Lymphoreticular infiltration in human tumours: prognosis and biological implications: a review. *Br J Cancer* 1974;30:538-548.
- Steele RJC, Brown M, Eremin O. Characterisation of macrophages infiltrating human mammary carcinomas. *Br J Cancer* 1985;51:135-138.
- Wood GW, Gollahon KA. Detection and quantitation of macrophage infiltration into primary human tumors with the use of cell-surface markers. *J Natl Cancer Inst* 1977;59:1081-1086.
- Brocker E-B, Zwadlo G, Suter L, Brune M, Sorg C. Infiltration of primary and metastatic melanomas with macrophages of the 25F9-positive phenotype. *Cancer Immunol Immunother* 1987;25:81-86.
- Schneider J, Hofman FM, Apuzzo MLJ, Hinton DR. Cytokines and immunoregulatory molecules in malignant glial neoplasms. *J Neurosurg* 1992;77: 265-273.
- Rossi ML, Cruz-Sanches F, Hughes JT, et al. Mononuclear cell infiltrate and HLA-DR expression in low grade astrocytomas. An immunohistological study of 23 cases. *Acta Neuropathol* 1988;76:281-286.
- Roessner A, Zwadlo G, Vollmer E, Sorg C, Grundmann E. Biologic characterization of human bone tumors IX. Occurrence of macrophages. *Pathol Res Pract* 1987;182:336-343.
- Matsumoto T, Iijima T, Kuwabara N, et al. Papillary renal cell carcinoma. Report of two cases. *Acta Pathol Jpn* 1992;42:298-303.
- Morra B, Ferrero V, Bussi M, Pacchioni D, Cerrato M, Bussolati G. Peri and intratumoral macrophage infiltration in laryngeal carcinoma. An immunohistochemical study. *Acta Otolaryngol Stockh* 1991;111:444-448.
- Lechleitner M, Gattringer C, Gastl G, et al. Macrophage infiltration in non-Hodgkin's lymphomas: a quantitative in situ study. *Immunobiology* 1986;171:381-387.
- Parham D, Whitaker JN, Berard CW. Cellular distribution of cathepsin D in childhood tumors. *Arch Pathol Lab Med* 1985;109:250-255.
- Graves DT, Valente AJ. Monocyte chemotactic proteins from human tumor cells. *Biochem Pharmacol* 1991;41:333-337.
- Shimosato Y. Histopathological studies on irradiated lung tumors. *Jpn J Cancer Res (Gann)* 1964;55:521-535.
- Ullrich RL, Casarett GW. Interrelationship between the early inflammatory response and subsequent fibrosis after radiation exposure. *Radiat Res* 1977; 72:107-121.
- Haberkmorn U, Strauss LG, Dimitrakopoulou A, et al. PET studies of fluoro-deoxyglucose metabolism in patients with recurrent colorectal tumors receiving radiotherapy. *J Nucl Med* 1991;32:1485-1490.
- Kaczmarek L, Kaminska B, Messina L, et al. Inhibitors of polyamine biosynthesis block tumor necrosis factor-induced activation of macrophages. *Cancer Res* 1992;52:1891-1894.
- Egenhart R, Kimming BN, Strauss LG, et al. Therapy monitoring of presacral recurrences after high-dose irradiation: value of PET, CT, CEA and pain score. *Strahlenther Onkol* 1992;168:203-212.

30. Kubota K, Kubota R, Matsuzawa T. Dose-responsive growth inhibition by glucocorticoid and its receptors in mouse teratocarcinoma OTT6050 in vivo. *Cancer Res* 1983;43:787-793.
31. Kubota K, Ishiwata K, Kubota R, et al. Tracer feasibility for monitoring of tumor radiotherapy: a quadruple-tracer study with ^{18}F -FDG or ^{18}F -FdUrd, ^{14}C -Met, ^3H -Thd and ^{67}Ga . *J Nucl Med* 1991;32:2118-2123.
32. Kubota K, Matsuzawa T, Takahashi T, et al. Rapid and sensitive response of carbon-11-L-methionine tumor uptake to irradiation. *J Nucl Med* 1989; 30:2012-2016.
33. Nathan CF. Secretory products of macrophages. *J Clin Invest* 1987;79:319-326.
34. Bustos R, Sobrino F. Stimulation of glycolysis as an activation signal in rat peritoneal macrophages. *Biochem J* 1992;282:299-303.

ERRATUM

DECEMBER FIRST IMPRESSIONS



ACQUISITION INFORMATION

A young woman was referred for a gastric emptying study. Conjugate images of the abdomen were sequentially acquired for 2 min each every 15 min after the oral ingestion of a 300-kcal meal labeled with $^{99\text{m}}\text{Tc}$ -sulfur colloid. A transmission scan was inadvertently superimposed on the 30-min images. These transmission artifacts were caused by radioactivity emanating from another patient who had been injected with approximately 28 mCi of $^{99\text{m}}\text{Tc}$ -methylene diphosphonate in the next room. He was lying up against the other side of a dry wall less than 6 feet from the woman having the gastric emptying study.

The transmitted activity is most intense between her hour-glass shaped torso and her arms. Transmission through the lungs is less intense. Most of the activity through the abdomen was attenuated. The emission

images of her stomach and small intestine were produced by the activity she ingested.

EMISSION IMAGE TRACER

Technetium-99m-sulfur colloid

TRANSMISSION IMAGE TRACER

Technetium-99m-methylene diphosphonate

TIME AFTER INGESTION

30 min

INSTRUMENTATION

GE Medical Systems Starcam 2000

CONTRIBUTOR

P. David Mozley

INSTITUTION

University of Pennsylvania, Philadelphia, Pennsylvania